The Modular Microarchitecture of Human Liver

Harald F. Teutsch

The morphological homogeneity of the liver parenchyma has represented a major obstacle in finding an acceptable definition of the structural/functional units of the liver. Concepts such as the "lobule," the "portal unit" and the "acinus" remain debatable. This study investigates the modular microarchitecture on the basis of the lobular concept. Using alkaline phosphatase activity as a histochemical marker, modules could be recognized clearly. In autopsy specimens of human liver, modules were traced through sequential cryosections, and a "secondary" module having a height of 1.9 mm, a surface of 14.7 mm^2, and a volume of 5.1 mm^3 was reconstructed three-dimensionally. It was subdivided into 14 "primary" modules by portal tracts and vascular septa and by a common draining central venular tree. Primary modules were polyhedral, with seven to nine facets, having heights from 0.3 to 0.9 mm, surface areas from 1.7 to 5.0 mm^2, and volumes from 0.1 to 0.9 mm^3. Such variation in shape and size is considered an important part of the modular organization of the human liver. In conclusion, the findings on the three-dimensionality and microcirculation of liver modules support and extend the lobular concept and, at the same time, make apparent the shortcomings of the concepts of acinar and portal units. The results of this study should permit a better interpretation of histological sections of normal and pathological liver and provide a basis for understanding the metabolic heterogeneity of liver cells and their functional integration into parenchymal units. (HEPATOLOGY **2005;42:317-325.**)

Since the first reports of a lobular subdivision of the liver in the 17th century,[1,2] various organizational concepts have been proposed,[3-15] and two conflicting models are still being used: the lobular unit,[3,4] in which blood is supplied to the surface and drained from the center, and portal and acinar units,[5-7] in which the supplying vessels are at the center and draining vessels on the surface. In rat liver, the demonstration of "lobular" units using glucose-6-phosphatase as a marker[16-18] led to the reconstruction of a secondary unit consisting of 14 primary units.[19] Recently, we reported on considerable degrees of variability in the shape and size of primary units as well as in the number of primary units integrated into secondary units in rat liver and used the term "modular microarchitecture" to describe this variability.[20] In the human liver,[9,21] three-dimensional reconstruction has provided detailed information on the lobular microvasculature, particularly on the vascular septum,[3,22-24] which connects portal venules and forms a continuous vascular surface from which sinusoids originate. Structural differences occur among sinusoids depending on their site of origin. In the rat liver, these structural differences are correlated with the metabolic heterogeneity of hepatocytes,[16-18] leading us to differentiate between "portal" and "septal" sinusoids. Matsumoto and colleagues[9,21] also reported on the subdivision of lobular "secondary units" into "primary units." Without a suitable marker, however, the borders of the primary units could be determined only on the surface of the secondary unit. It was not possible to assess the shapes or sizes of the primary units or the internal subdivision of the secondary unit. Therefore, in the present study, alkaline phosphatase activity was used as a marker for three-dimensional reconstruction to investigate the modular microarchitecture of the human liver.

Materials and Methods

Preparation of Materials. Human liver specimens were obtained from the Department of Pathology of the University of Ulm. Tissue was collected during routine autopsy and after surgical removal of solitary tumor metastases of the liver. Liver tissue was frozen and stored in

From the Department of Anatomy and Cell Biology, University of Ulm, Ulm, Germany.

Received December 22, 2004; accepted May 4, 2005.

Supported by a grant from the Deutsche Forschungsgemeinschaft (Te 75/6-1, 75/6-2).

Address reprint requests to: Prof. Dr. Harald F. Teutsch, Department of Anatomy and Cell Biology, University of Ulm, Albert-Einstein Allee 11, D-89069 Ulm, Germany. E-mail: harald.teutsch@uni-ulm.de; fax: (49) 731-500-23214.

Copyright © 2005 by the American Association for the Study of Liver Diseases.

Published online in Wiley InterScience (www.interscience.wiley.com).

DOI 10.1002/hep.20764

Potential conflict of interest: Nothing to report.

liquid nitrogen. Tissue samples were trimmed and marked so that the outlines of the sections could be used for the vertical orientation of the section planes. The study protocol conformed to the ethical guidelines of the 1975 Declaration of Helsinki, as reflected by the *a priori* approval (no. 18/2001) of the ethics commission of the medical faculty of the University of Ulm.

Histochemical Demonstration of Alkaline Phosphatase, E.C.3.1.3.1. Serial sections (14 μm) were cut parallel to the organ surface at −20°C, air-dried for 5 minutes at 37°C, and fixed at 4°C for 1 minute in a solution containing HEPES-NaOH buffer (100 mmol/L; pH 7.4), glutaraldehyde (1.25%), and saccharose (1%). Enzyme activity was demonstrated according to Burstone[25] using a staining kit (SK 5200, Vectastain ABC-AP; Vector Laboratories, Burlingame, CA). Cell nuclei were stained with Mayer's hemalum.[26] Incubation of sections in a medium containing 0.5 mmol/L levamisole resulted in inhibition of most of the enzyme activity.

Three-Dimensional Reconstruction. From several series of sections from tissue samples of four different livers, one series of a total of 559 sections (autopsy sample 34310/92 from the right lobe of the liver of a 59-year-old man) was used for reconstruction. Because of the complexity of three-dimensional reconstruction, the present study was restricted to a single secondary module. The images were photographed at a magnification of ×12.5, scanned at high resolution into Photoshop 7.0 (Adobe Systems Inc., San Jose, CA), and oriented vertically using the section outlines. Drawings of the images were imported into "Surfdriver" (David Moody and Scott Lozanoff, 1999; http://www.surfdriver.com) for reconstruction. Topographically, the secondary module extended from 4.5 mm to 6.4 mm below the organ surface. Physical models were built at a magnification of 75:1, as previously described.[19]

Morphometric Analyses. The drawings of alternating section planes were imported into Axiovision 3.1 (Zeiss, Oberkochen, Germany) for morphometric measurements.

Results and Discussion

Distribution of Alkaline Phosphatase Activity. The enzyme is known to occur in variable activity in the endothelium of portal and central veins, hepatic arteries, sinusoids, and bile canaliculi.[27,28] For reconstruction, we chose a tissue specimen in which the endothelium of portal and central veins and sinusoids was clearly marked, so that the relevant structural elements of the modular microarchitecture could be identified. Fig. 1 shows a cross-section of a secondary module, which is composed of primary modules (Ia, IIb-VIb). At the surface of the modules, areas of high enzyme activity mark endothelial cells of portal veins and of the initial tortuous segment of portal sinusoids that originate directly from and in the vicinity of the portal veins (Fig. 1A-B; red arrows in module Ia and IIb). Between neighboring portal veins, where blood is distributed along interconnecting vascular septa, en-

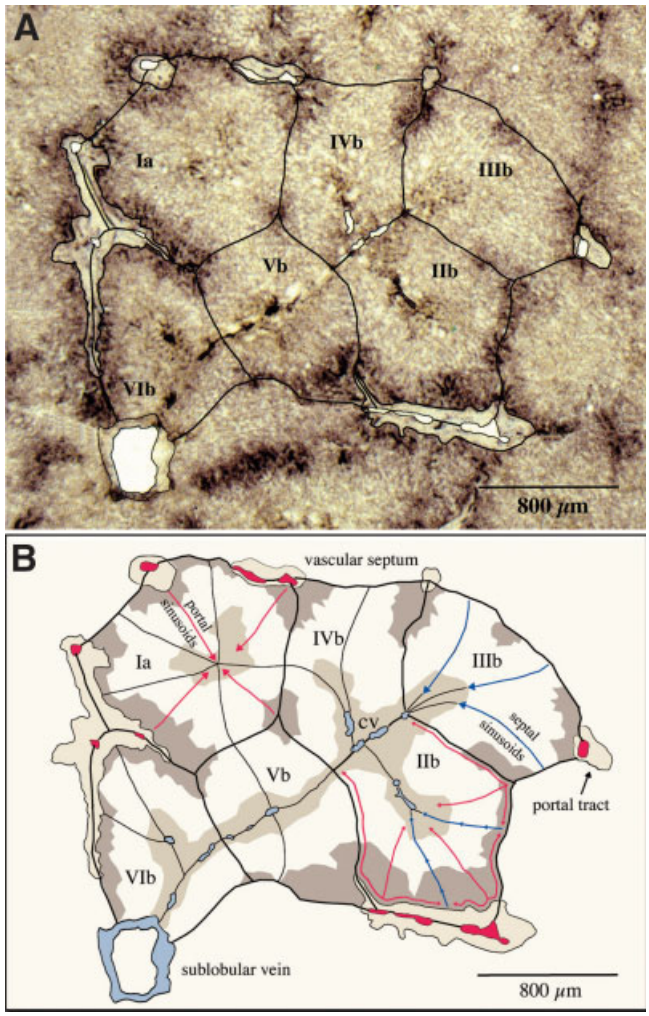

Fig. 1. Distribution of alkaline phosphatase activity. Portal venular branches and vascular septa form a continuum in which blood is distributed over the surface of the modules and from which the sinusoids originate (black lines). From portal vessels, blood flows toward the center and along the vascular septa (module IIb, red and blue arrows). Enzyme activity was highest in endothelial cells at the beginning of "portal" sinusoids (module Ia, red arrows). From there, activity decreased toward the central venule and was higher at the end of the sinusoids. Staining also decreased from both sides along the vascular septum and was lowest where the "septal" sinusoids originate (module IIIb, blue arrows). Along septal sinusoids, alkaline phosphatase activity first decreased and then increased toward the end of the sinusoids. Panel B shows the portal tracts (light brown) and branches of the portal vein (red) connected by vascular septa (black lines), portal areas (dark brown), comprising initial segments of the sinusoids, with high enzyme activity, central areas (light brown), comprising the terminal segment of sinusoids, with high enzyme activity, central venules (blue), and borders between inflow sources. cv, central venules.

zyme activity decreased from both sides and was lowest where the flow-fronts meet and septal sinusoids originate (Fig. 1B; blue arrows in module IIb and IIIb). The areas of high enzyme activity at the surface of the modules (Fig. 1B; areas shaded in dark gray) correspond to the "sickle zones,"[9,21] the lateral ends of which meet where septal sinusoids originate. In direction of blood flow—that is, from the transition of the tortuous into the straight segment of portal sinusoids and from the origin of the straight septal sinusoids—enzyme activity first decreased and then increased toward the end of the sinusoids at the central veins (Fig. 1A-B; central areas shaded in light gray). Although little is known about the specific function of hepatic alkaline phosphatase,[29] the heterogeneity of sinusoidal endothelial cells correlates with structural differences among sinusoids of different origin[9] and thus supports a differentiation of "portal" and "septal" sinusoids in human liver.[16-18]

General Organization of the Parenchyma. Reconstruction revealed a group of 14 primary modules integrated into a secondary module (Fig. 2). Integration resulted from a common drainage by the branches of a central venular tree (Figs. 3, 4A) and from the arrangement of portal venular branches and vascular septa, which form a continuous vascular surface over the entire module and separate it from adjacent modules (Figs. 2, 3). The secondary module had a height of 1.862 mm, a surface area of 14,666 mm^2, and a volume of 5.146 mm^3. The maximum length and width were 3.463 and 3.355 mm, respectively. With the exception of modules Vc and Vd, primary modules were arranged in two horizontal layers (Figs. 3, 5): a top layer comprising modules Ia to VIa and a bottom layer composed of modules Ib to VIb. Additionally, the modules were arranged in six vertical groups (Figs. 3 [right column], 4A, 6, 7): 5 groups of two modules each (Ia/b, IIa/b, IIa/b, IVa/b, and VIa/b), and one group of 4 modules (Va-d). Group VI was located next to the draining sublobular vein (Fig. 3, right column), followed by groups I and V, in an opposing position, and by groups IV and II, also in an opposing position, adjacent to group III. This assembly is quite different from that of rat liver,[19,20] in which modules are stacked along a vertical axis.

The Central Venular Tree. Primary modules were drained by a single branch of the central venular tree (Fig. 4A), which was located in the center and oriented along the vertical axis of the modules, as well as by occasional additional smaller branches (not shown). The diameter of the branches varied between 11 ± 2 (±SEM) μm at the distal beginning and 57 ± 4 μm at the central end where branches fused. These diameters are smaller than those seen in rat liver, which ranged from 62 ± 14 μm to 216 ± 9 μm,[19] as was the number of branching steps (2 in human liver and 4 in rat liver). Tracing the central venular tree and its branches[19] revealed which of the primary modules were part of a particular secondary module and where individual modules ended (*i.e.*, the fusion of central veins). The central areas of high enzyme activity (Figs. 1, 2, and 3 [right column]) were also used for tracing individual modules, because they extended throughout a larger portion of the modules. Following the direction of blood flow (Fig. 4A, arrowheads), the central veins of modules IIIa/b, IVa/b, IIa/b and Va/b joined and connected in order from left to right to the adjacent central veins. The fusion of most of the central veins occurred in a narrow horizontal plane (planes 43-49): the central veins of modules Va and Vb joined and connected to

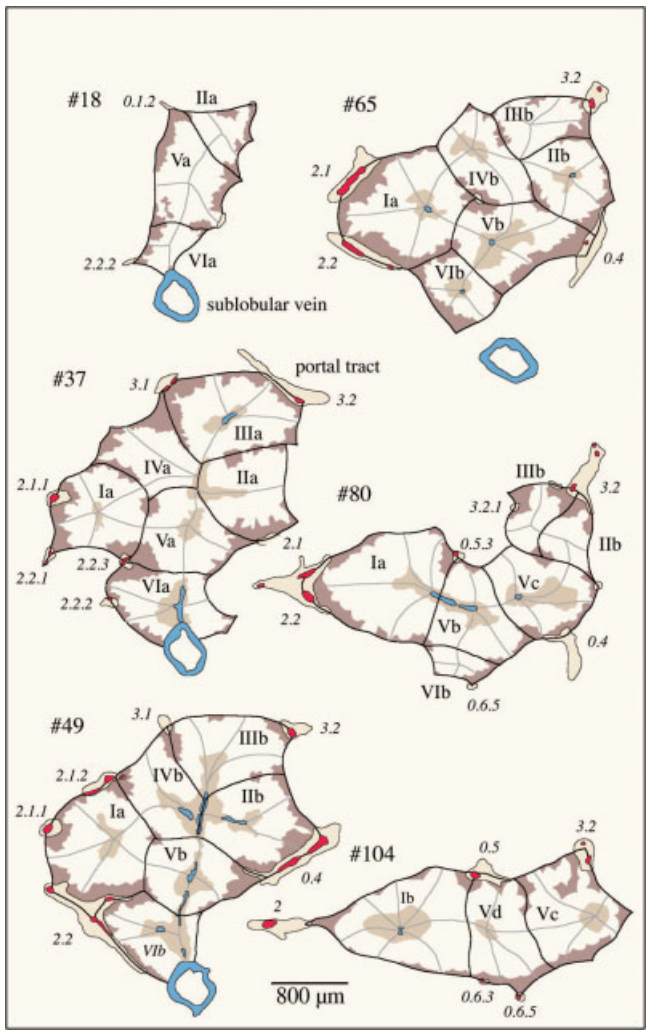

Fig. 2. Representative section planes 18, 37, 49, 65, 80, and 104. Each panel shows the secondary module and its subdivision by portal veins (marked by italic numerals), vascular septa, and branches of the central venular tree into primary modules. The drawings comprise information for reconstruction, as described for Fig. 1B. Gray lines indicate borders between inflow fronts.

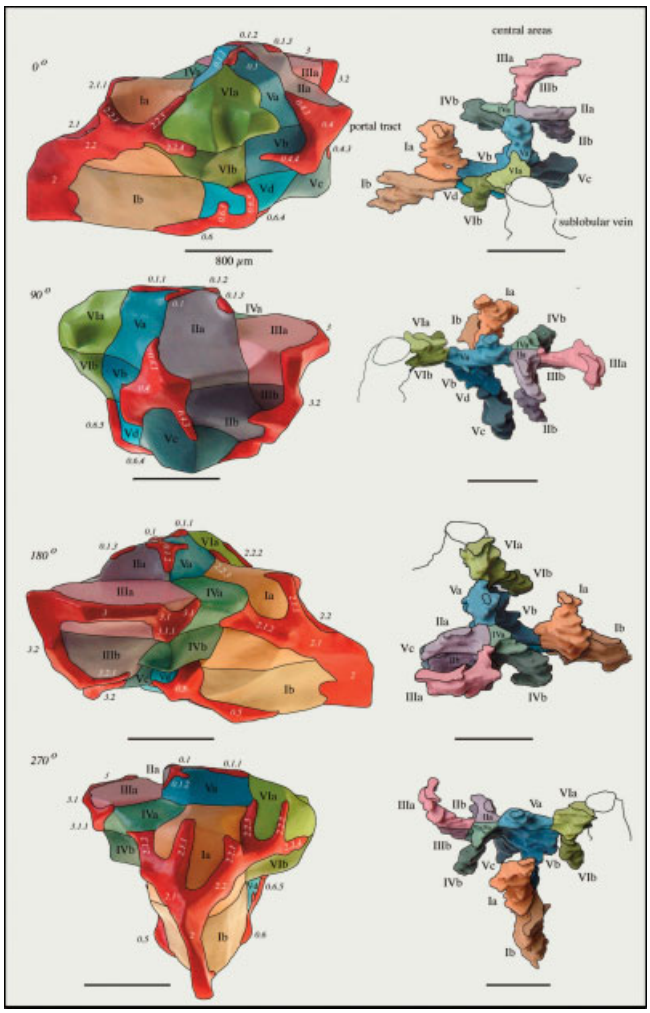

Fig. 3. Reconstruction of the secondary module and its "central areas." The secondary module is shown on the left and its central areas on the right. Front view (0°) and views after turning clockwise 90°, 180°, and 270° are represented. Primary modules and corresponding central areas are color-coded and marked by Roman numerals. Portal tracts (red) are identified by Arabic numerals. The sublobular vein drains the secondary module.

those of modules VIa and VIb, which emptied into the sublobular vein. The fusion of the central veins of modules Vc and Vb occurred in section plane 74. The central veins of modules Ia and Ib were connected to that of module Vb (planes 80-83). The central venular tree had a horizontal main axis and two perpendicular axes (Fig. 3 [right column]), resulting in a shape that was quite different from that reconstructed in rat liver,[19] where the branches and the branching steps were oriented preferentially along a vertical axis.

Portal Venous Trees. The secondary module was supplied by six portal veins (Figs. 3 [left column], 4B). According to the branching pattern, three types of branches could be distinguished (Fig. 4B): 2 type 1 vessels (Fig. 4B [2, 3]) with an average diameter of 55 ± 3 (±SEM) μm; 8 type 2 branches with a diameter of 47 ± 2 μm (Fig. 4B [0.6, 0.5, 2.2, 2.1, 0.4, 0.1, 3.1, and 3.2]); and 24 type 3 branches with a diameter of 26 ± 1 μm. Of a total of 34 portal venular branches, 31 were located on the surface of the secondary module, and only 3 supplied blood to the "internal" surfaces of the primary modules (Fig. 4B [0.6.2, 0.5.3, 0.4.2]). Matsumoto and colleagues[9,21] have described a similar three-step branching. Third-step septal branches, in their course, lose their connective tissue sheets, their wall structure resembles that of the sinusoids, and they can then be recognized only by their "interlobular" location and larger lumina. In our study, the "proximal" part of the septal branches could be traced directly, while the "distal" sinusoid-like part was identified by areas of high alkaline phosphatase activity along the vascular septa (Figs. 6 and 7, red lines).

Organization of the Secondary Module. A total of six groups of primary modules were integrated into a secondary module. Five groups consisted of two primary modules, and one group (group V) consisted of 4 primary modules each (Figs. 3, 5, 6, and 7). In the following discussion, group I and modules Ia and Ib are described in

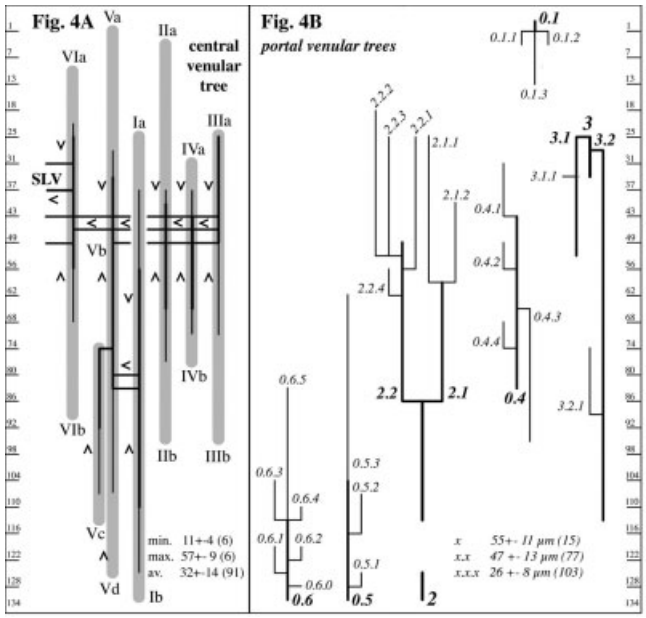

Fig. 4. (A) The central venular tree. Vertical scale: section planes. Gray shading: extension of the primary modules (Roman numerals). Thin black lines: central areas of high enzyme activity. Thick black lines indicate branches of the central venular tree; arrowheads, direction of blood flow; and SLV, where the central venular tree connects to the sublobular vein. Min., max., av.: minimal, maximal, and average diameters of central venular branches (±SEM) (number of measurements appears in parentheses). (B) Portal venular trees. The 6 supplying portal venular trees, with 3 types of branches: main branches (single number), first-step ramifications (two numbers), and second-step ramifications (three numbers). X, x.x, x.x.x: mean values ± SEM of the diameters of main and first- and second-step branches, respectively (number of measurements appears in parentheses).

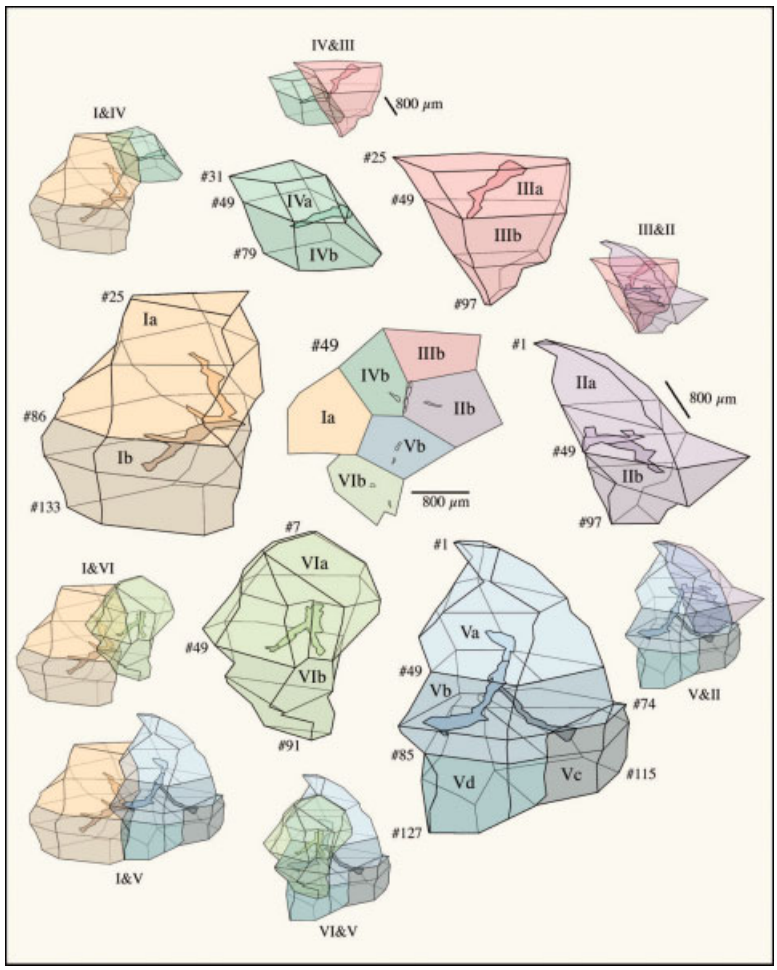

Fig. 5. Organization of the secondary module. Center: cross-section (plane 49) of the secondary module and its primary modules. Panels at the center: six groups of primary modules (Ia/b, IVa/b, IIIa/b, IIa/b, Va-d, and VIa/b). Numerals at the left side of the panels: section planes, where modules begin and end. Contours in the center of the primary modules: branches of the central venular tree. Other smaller panels: neighboring groups of primary modules.

detail. Information on the other groups and the primary modules is presented in Figs. 2, 3, 5, 6, and 7 and in Table 1.

Group I (Figs. 5, 6) consisted of two primary modules (Ia and Ib) that opposed each other with respect to the direction of central venular blood flow. This group was located on the left side of the secondary module. The blood supply (Fig. 6 [left column]) came from portal veins 2, 0.5, 0.6 and their branches (Fig. 4B). Distal portions of septal branches (Fig. 6 [left column], red lines) were identified based on the distribution of areas of high alkaline phosphatase activity on the vascular surface of the modules (Figs. 1A [IB], 2). This is indicated in Fig. 6 by darker shading of the surface. Analysis of the blood supply by portal veins and septal branches revealed the different vascular septa, the direction of blood flow (Fig. 6, red arrows on the surface of the modules) and where along the individual septa flow-fronts from neighboring inflow sources meet (violet lines) and septal sinusoids originate. This location corresponds to the border between adjacent "sickle-zones."[9,21]

Module Ia (Figs. 5, 6) had a total of 8 facets. It had a height of 896 μm, a volume of 0.890 mm^3, and a surface area of 5.013 mm^2 (Table 1). Its surface was subdivided into 5 vascular septa with areas from 0.492 to 0.808 mm^2. The apparent length of portal sinusoids was 654 $\pm$ 20 ($\pm$SEM) μm; and the apparent length of septal sinusoids was 557 $\pm$ 11 μm. The module was drained by one central vein (and a smaller side branch), which fused with that of module Ib in planes 88/89 and emptied here into the central veins of modules Vb and Vd (Fig. 6 [90° view]).

Module Ib had 8 facets. It was 630 μm high and had a volume of 0.659 mm^3 and a surface area of 4.907 mm^2. The surface was subdivided into 7 septa, with areas between 0.191 and 0.680 mm^2. The apparent length of portal sinusoids was 666 $\pm$ 23 ($\pm$SEM) μm; the apparent length of septal sinusoids was 545 $\pm$ 17 μm. Module Ib was drained by one central vein and a smaller side branch (Fig. 5). The central vein fused with that of module Ia and emptied into the joined central veins of modules Vb and Vd.

Conclusions. To investigate the modular microarchitecture of hepatic parenchyma, the problem of morphological homogeneity, which conceals the liver's internal organization, had to be resolved. This was accomplished

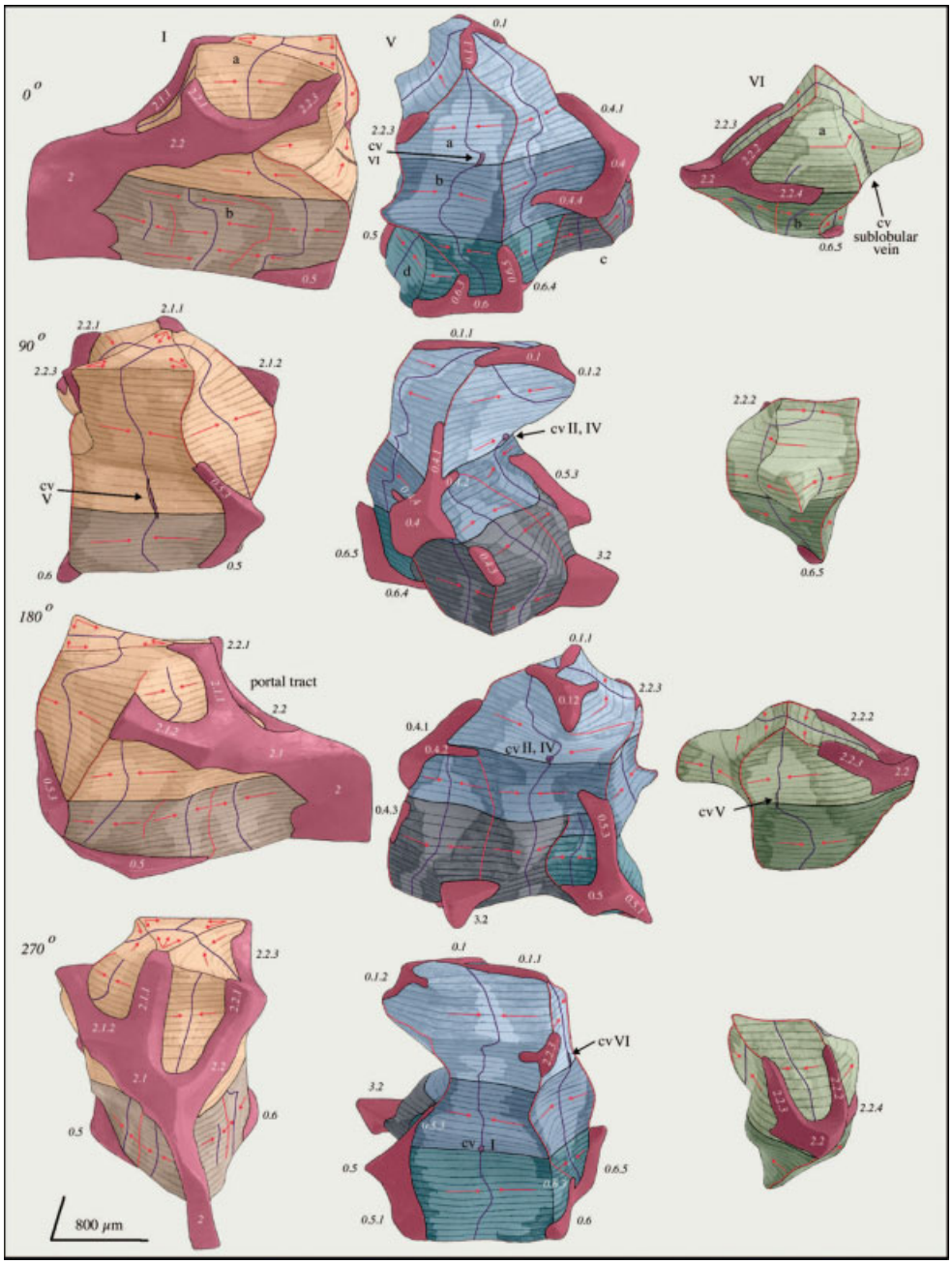

Fig. 6. Groups I, V, and VI of primary modules. Front view (top row) and views after turning clockwise for 90°, 180°, and 270° are represented. Groups I and VI consist of two primary modules each (a, b). Group V consists of four primary modules (a-d). The abbreviation "cv" indicates the position at which the central venular branch connects to those of neighboring primary modules (Roman numerals). In group VI, the arrow indicates where the central venular tree is connected to the sublobular vein. Black lines: borders between primary modules, identified by letters. Primary modules are colored as in Fig. 3; areas of high enzyme activity at the beginning of sinusoids are shaded darker. Portal tracts: red. Red lines: septal branches of portal veins. Red arrows: direction of blood flow. Violet lines show where inflow-fronts meet and where septal sinusoids originate.

using a metabolic marker rather than a histological staining procedure.[9] Alkaline phosphatase activity was chosen because of its unique distribution in endothelial cells of the human liver, which allows the relevant structural elements of the modules to be clearly identified. The unusual stability of this enzyme[27,28] is also of advantage, because it permits the use of autopsy samples.

Using this approach, we confirmed and extended the results of Matsumoto and Kawakami's study on the lobular organization of human liver.[9] The secondary module we reconstructed is larger than the secondary unit they described and is composed of 14 rather than 7 primary units. While Matsumoto and Kawakami's primary units were not reconstructed but were assumed to be cone-shaped, our reconstructed modules were polyhedral, with 7 to 9 facets, which are either plane, convex, or concave. In addition to variable shapes, the primary modules also varied in size (*i.e.*, height, surface area, volume, number and area of vascular septa). Such morphogenetic plasticity is considered an important part of the modular microarchitecture of the liver.

Our findings also allowed for a critical reappraisal of Matsumoto and Kawakami's conclusion that their secondary unit correlates with a "classical lobule."[9] Primarily because of the size of the secondary unit and the branching of the central venular tree (see Figs. 12 and 13 in

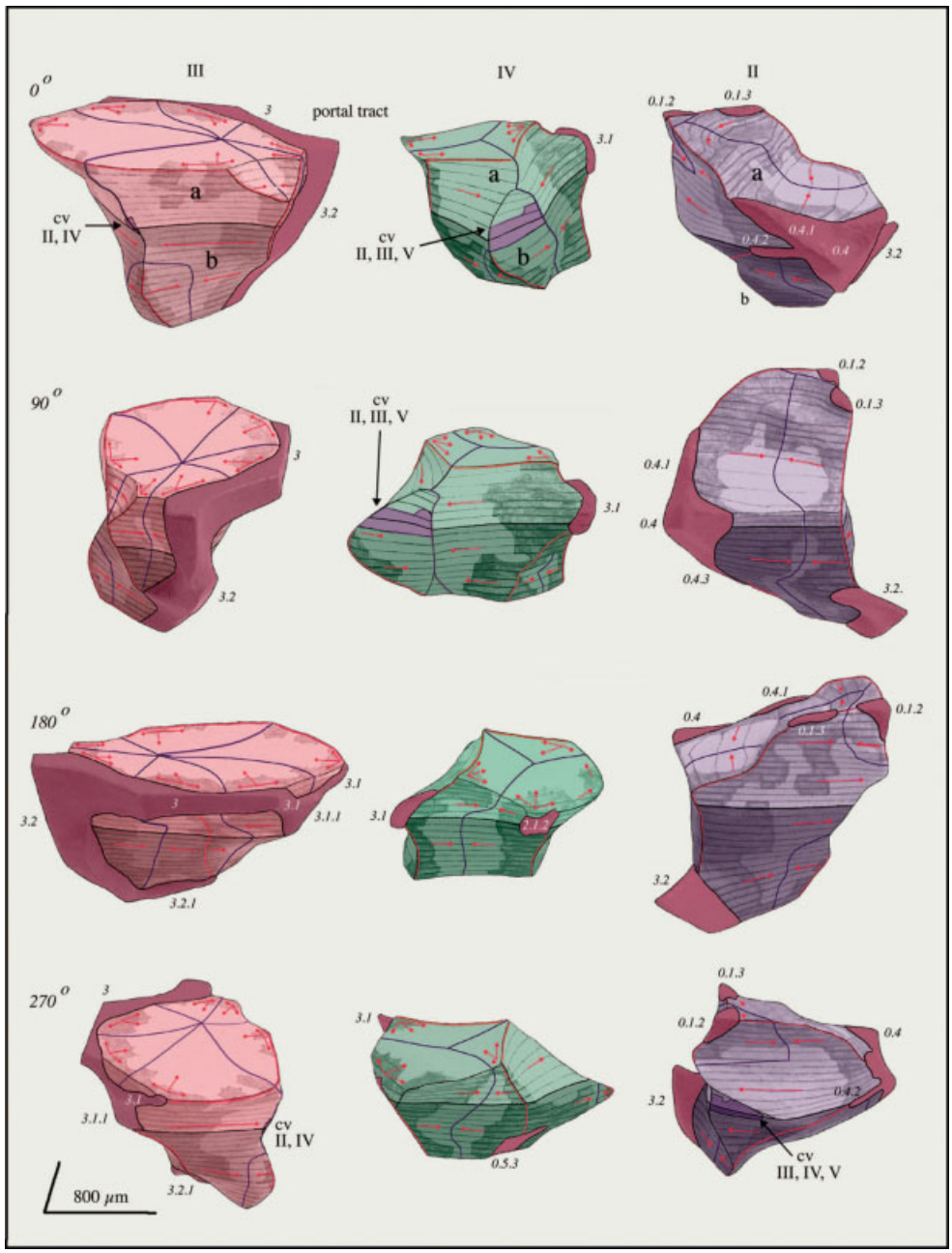

Fig. 7. Groups III, IV, and II of primary modules. Front view (top row) and views after turning clockwise for 90°, 180°, and 270° are represented. Groups III, IV, and II consist of two primary modules each (a, b). The abbreviation "cv" indicates the position at which the central venular branch connects to those of neighboring primary modules (Roman numerals). Black lines: borders between primary modules, identified by letters. Primary modules are colored as in Fig. 3; areas of high enzyme activity at the beginning of sinusoids are shaded darker. Portal tracts: red. Red lines: septal branches of portal veins. Red arrows: direction of blood flow. Violet lines show where inflow-fronts meet and where septal sinusoids originate.

Matsumoto and Kawakami's paper[9]) we conclude that it is not the secondary but rather the primary units that correlate with "classical lobules." Such assembly of primary modules into secondary modules then becomes comparable to that seen in rat[19,20] and pig liver.[30,31]

Primary modules of human and rat liver[9,19,20] share similar structural elements that are responsible for directing and timing of blood flow: (1) portal veins and their septal branches (and hepatic arteries); (2) vascular septa, which connect portal veins and septal branches to a continuous supplying surface and act as a "watershed" between adjacent primary modules[9]; (3) long portal sinusoids, which originate directly from and in the vicinity of the portal vessels, with an initial tortuous segment and a subsequent straight radially oriented segment; (4) short septal sinusoids, which are straight radial and lacking the initial tortuous segment that originate from the vascular septum, where inflow-fronts from neighboring portal vessels meet; and (5) a central venular branch located in the center of the primary module, draining the sinusoids.

There are also differences between the human and rat liver[19]: the shape of the primary modules is more complex in human than in rat liver; primary modules are arranged differently within the secondary module; portal and septal sinusoids in average are longer by 205 and 124 μm, respectively; the branching pattern of the central venular

Table 1. Morphometric Analyses

Group	Blood Supply (Portal Veins)	Module	Facets	Height (μm)	Volume (mm^3)	Surface Area (mm^2)	Areas of Vascular Septa, mm^2 (Number of Septa)	Length of Portal Sinusoids (μm), ± SEM*	Length of Septal Sinusoids (μm), ± SEM*
I	2, 2.1, 2.1.1, 2.1.2, 2.2, 2.2.1	Ia	8	896	0.890	5.013	0.492; 0.556; 0.808; 0.755; 0.803 (5)	654 ± 20 (104)	557 ± 11 (100)
	2.2.3, 0.5, 0.5.3, 0.6, 0.6.0	Ib	8	630	0.659	4.907	0.680; 0.337; 0.264; 0.267; 0.505; 0.515; 0.191 (7)	666 ± 23 (89)	545 ± 17 (89)
II	0.1.2, 0.1.3, 0.4, 0.4.1, 0.4.2	IIa	7	630	0.263	2.576	0.518; 0.619; 0.572 (3)	632 ± 43 (39)	393 ± 57 (31)
	0.4.3, 0.3.2	IIb	7	686	0.309	2.680	0.229; 0.622; 0.398; 0.119; 0.382 (5)	525 ± 27 (49)	368 ± 24 (49)
III	3, 3.1, 3.1.1, 3.2, 3.2.1	IIIa	7	364	0.348	3.352	0.167; 0.114; 0.239; 0.053; 0.147; 0.286; 0.286 (7)	721 ± 26 (40)	593 ± 27 (39)
		IIIb	9	658	0.282	2.572	0.305; 0.274; 0.124; 0.546; 0.525 (5)	573 ± 32 (57)	428 ± 37 (53)
IV	2.1.2, 3.1, 0.5.3	IVa	8	252	0.132	1.708	0.157; 0.265; 0.403 (3)	623 ± 55 (18)	543 ± 58 (15)
		IVb	8	434	0.259	2.305	0.272; 0.279; 0.450; 0.251; 0.091 (5)	525 ± 22 (46)	424 ± 21 (46)
V	0.1, 0.1.1, 0.1.2, 2.2.3, 3.2,	Va	7	672	0.368	2.849	0.263; 0.372; 0.571; 0.340; 0.495 (5)	576 ± 24 (61)	400 ± 19 (61)
	0.4, 0.4.1, 0.4.2, 0.4.3, 0.4.4	Vb	8	518	0.372	3.314	0.465; 0.385; 0.402; 0.326; 0.196; 0.158 (6)	578 ± 22 (59)	430 ± 19 (59)
	0.5, 0.5.1, 0.5.2, 0.5.3	Vc	9	588	0.415	3.062	0.241; 0.449; 0.396; 0.358; 0.561 (5)	590 ± 19 (70)	474 ± 20 (70)
	0.6.1, 0.6.3, 0.6.4, 0.6.5	Vd	8	588	0.388	3.118	0.180; 0.705; 0.219; 0.305; 0.604 (5)	594 ± 17 (62)	450 ± 22 (62)
VI	2.2, 2.2.2, 2.2.3, 0.6.5	VIa	9	546	0.237	2.728	0.265; 0.383; 0.943; 0.326; 0.163 (5)	525 ± 21 (47)	364 ± 29 (45)
		VIb	8	602	0.224	2.149	0.610; 0.345; 0.309; 0.244 (4)	447 ± 20 (53)	331 ± 19 (53)
I-VI	Total height			1862				588 ± 19 (14)	450 ± 22 (14)
	Total volume				5.146				
	Outer surface					14.666			

*Numbers in parentheses indicate the number of measurements

tree is different; and the diameters of the branches of the central venular tree are considerably smaller in human liver compared with rat liver.

Whereas the vascular septum in human and in rat liver[9,19] has been shown to be essential for the distribution of blood to the entire surface of the primary modules, it is not compatible with the concepts of either the acinus[6-8] or the portal unit.[5] Blood flow through the acinar and portal units is very different, because both units are arranged around a central axis of blood supply, from which sinusoids are thought to diverge in all directions. From this it follows that sinusoidal blood has to be collected from a large surface into a small number of draining vessels.[19] Blood flow of the vascular septa, therefore, would cut through the middle of the acinar unit and separate the portal unit into three parts. In both concepts, sinusoidal blood supply is restricted to the terminal branches of the portal vein. This is not the case in either human[9] or rat liver[19] in which the portions of the portal venular tree supplying the sinusoids are much larger and comprise three generations of branches. Acinar or portal units, therefore, do not fit into the complex three-dimensionality of the portal venular tree.

In conclusion, knowledge of the three-dimensionality and microcirculation of primary and secondary modules can improve the interpretation of (two-dimensional) tissue sections from normal and, especially, pathologically altered liver tissue (*e.g.*, chronic congestion and cirrhosis.[9,19,21,32] It provides a new basis for progress in the understanding of the metabolic heterogeneity of liver cells[16-19] and its regulation.

Acknowledgment: The author is grateful to T. L. Kyander-Teutsch for the building of physical models of liver modules and morphometric measurements, to E. Groezinger for technical assistance with sectioning and histochemical staining, and to J. Baron, Ph.D., for assistance with the manuscript.

References

1. Wepfer JJ. De dubiis anatomicis. Epistola cum responsione. Norimberg, 1665.
2. Malpighi A. De viscerum structura. Exercitatio anatomica. London, 1666.
3. Kiernan F. The anatomy and physiology of the liver. Philos Trans R Soc Lond 1833;123:711-770.
4. Pfuhl W. Form und Gefaeßbeziehungen der Leberlaeppchen beim Menschen. Z Anat Entwicklgesch 1922;66:361-384.
5. Mall F. A study of the structural unit of the liver. J Anat 1906;5:227-308.
6. Rappaport AM, Borowy ZJ, Lougheed WM, Lotto N. Subdivision of hexagonal liver lobules into a structural and functional unit. Anat Rec 1954;119:11-34.
7. Rappaport AM. Physioanatomic considerations. In: Schiff L, Schiff ER, eds. Diseases of the Liver. Philadelphia: J.B. Lippincott Company, 1982: 1-52.
8. Sasse D. Liver structure and innervation. In: Thurmann RG, Kauffman FC, Jungermann K, eds. Regulation of Hepatic Metabolism. New York, London: Plenum Press, 1986:3-25.
9. Matsumoto T, Kawakami M. The unit-concept of hepatic parenchyma. A re-examination based on angioarchitectural studies. Acta Pathol Jpn 1982; (Suppl 2):285-314.
10. Quistorff B, Rømert P. High zone-selectivity of cell permeabilization following digitonin-pulse perfusion of rat liver. A re-interpretation of microcirculatory zones. Histochemistry 1989;92:487-498.
11. Lamers WH, Hilberts A, Furt E, Smith J, Jonges GN, van Noorden CJF, et al. Hepatic enzymic zonation: a reevaluation of the concept of the liver acinus. HEPATOLOGY 1989;10:72-76.
12. Rømert P, Quistorff B, Behnke O. Histological evaluation of the zonation of colloidal gold uptake by the rat liver. Tissue Cell 1993;25:19-32.
13. Ekataksin W, Zou ZZ, Wake K, Chunhabundit P, Somana R, Nishida J, et al. HMS, Hepatic microcirculatory subunits in mammalian species: intralobular grouping of liver tissue with definition enhanced by the drop-out sinusoids. In: Wisse E, Knook DL, Wake K, eds. Cells of the Hepatic Sinusoids. Volume 5. Leiden: Kupffer Cell Foundation, 1995:247-251.
14. Saxena R, Theise ND, Crawford JM. Microanatomy of the human liver—exploring the hidden interfaces. HEPATOLOGY 1999;30:1339-1346.
15. Desmet VJ. Organizational principles. In: Arias IM, Boyer JL, Chisari FV, Fausto N, Schachter D, Shafritz DA, eds. The Liver: Biology and Pathobiology. 4th ed. Philadelphia: Lippincott Williams & Wilkins, 2001:3-15.
16. Teutsch HF. Sex-specific regionality of liver metabolism during starvation; with special reference to the heterogeneity of the lobular periphery. Histochemistry 1984;81:87-92.
17. Teutsch HF. Regionality of glucose-6-phosphate hydrolysis in the liver lobule of the rat: metabolic heterogeneity of "portal" and "septal" sinusoids. HEPATOLOGY 1988;8:311-317.
18. Teutsch HF, Altemus J, Gerlach-Arbeiter S, Kyander-Teutsch TL. Distribution of 3-hydroxybyturate dehydrogenase in primary lobules of rat liver. J Histochem Cytochem 1992;40:213-219.
19. Teutsch HF, Schuerfeld D, Groezinger E. Three-dimensional reconstruction of parenchymal units in the liver of the rat. HEPATOLOGY 1999;29: 494-505.
20. Teutsch HF. Modular design of the liver of the rat. In: Malcom G, ed. Multidisciplinary Approaches to Visual Representations and Interpretations. Amsterdam: Elsevier Science, 2004:63-67.
21. Matsumoto T, Komori R, Magara T, Ui T, Kawakami M, Tokuda T, et al. A study on the normal structure of human liver, with special reference to its angioarchitecture. Jikeikai Med J 1979;26:1-40.
22. Debeyre A. Morphologie du lobule hépatique. Bibl Anat 1910;19:249-263.
23. Debeyre A. Circulation porte du lobule hépatique. Bibl Anat 1912;22: 189-225.
24. Pfuhl W. Die Leber. In: von Moellendorf, ed. Handbuch der mikroskopischen Anatomie des Menschen. Volume 5. Berlin: Springer Verlag, 1932:235-425.
25. Burstone MS. Enzyme histochemistry and its application in the study of neoplasms. New York: Academic Press, 1963.
26. Romeis B. Haematoxylin. In: Boeck P, ed. Romeis. Mikroskopische Technik. 17th ed. Muenchen: Urban & Schwarzenberg, 1989:214-219.
27. Haegerstrand I. Distribution of alkaline phosphatase activity in healthy and deseased human liver tissue. Acta Pathol Microbiol Scand A 1975;83: 519-526.
28. Haegerstrand I. Bile canalicular alkaline phosphatase in necropsy specimens of the liver and its relation to disease. Acta Pathol Microbiol Scand A 1976;84:278-284.
29. Zoellner HFA, Hunter N. Histochemical identification of the vascular endothelial isoenzyme of alkaline phosphatase. J Histochem Cytochem 1989;37:1893-1898.
30. Wuensche A. Leberlaeppchen und portale Gefaeßscheide beim Schwein. In: Vollmer haus B, ed. Advances in Veterinary Medicine. Supplements to Journal of Veterinary Medicine, Number 39. Berlin, Germany: Parey, 1988:1-117.
31. Ekataksin W, Wake K. Liver units in three dimensions. I. Organization of argyrophilic connective tissue skeleton in porcine liver with particular reference to the "compound hepatic lobule." Am J Anat 1991;191:113-153.
32. Wanless IR, Nakashima E, Sherman M. Regression of human cirrhosis. Morphological features and genesis of incomplete septal cirrhosis. Arch Pathol Lab Med 2000;124:1599-1607.